

Pharmacokinetic Analysis of Huangqi Guizhi Wuwu Decoction on Blood and Brain Tissue in Rats with Normal and Cerebral Ischemia-Reperfusion Injury by Microdialysis with HPLC-MS/MS

This article was published in the following Dove Press journal:
Drug Design, Development and Therapy

Hao-Zhen Zheng
Xiao Shen
Ying-Ying He
Xiang-Li Yan
Sheng-Xin Wang
Ai-Ming Yu
Li-Sheng Wang

College of Chinese Materia Medica,
Guangzhou University of Chinese
Medicine, Guangzhou 51006, Guangdong,
People's Republic of China

Objective: The aim of our research was to analyze and compare the pharmacokinetics of paeoniflorin, calycosin, calycosin-7-o- β -d-6-glucoside, and 6-gingerol in the blood and brain tissue of normal and cerebral ischemia-reperfusion injury rats by HPLC-MS/MS method.

Methods: The blood and brain tissue samples of normal and middle cerebral artery occlusion (MCAO) rats were compared. The blood and brain tissue samples were collected by using microdialysis technique. The concentrations of paeoniflorin, calycosin, calycosin-7-o- β -d-6-glucoside, and 6-gingerol in blood and brain tissues were determined by the HPLC-MS/MS internal standard method.

Results: Compared with the normal group, the model group after the administration of the Huangqi Guizhi Wuwu Decoction showed that $C_{\max \text{ blood}}$, $AUC_{0-t \text{ blood}}$, and $AUC_{0-inf \text{ blood}}$ of paeoniflorin were increased, CL_{blood} , $t_{1/2 \text{ brain}}$, and V_{brain} of paeoniflorin were decreased; $C_{\max \text{ blood}}$, $AUC_{0-t \text{ blood}}$, $AUC_{0-inf \text{ blood}}$, and average residence time (MRT_{brain}) of calycosin-7-o- β -d-6-glucoside were decreased and the CL_{blood} and $C_{\max \text{ brain}}$ of calycosin-7-o- β -d-6-glucoside were increased; $C_{\max \text{ blood}}$ of calycosin was decreased, V_{blood} and V_{brain} of calycosin were increased; $C_{\max \text{ blood}}$, $AUC_{0-t \text{ blood}}$, $AUC_{0-inf \text{ blood}}$, and MRT_{brain} of 6-gingerol were decreased, CL_{blood} of 6-gingerol was increased.

Conclusion: This method is simple, rapid, and sensitive. It is suitable for the pharmacokinetic study of Huangqi Guizhi Wuwu Decoction in the blood and brain tissue of rats. Cerebral ischemia-reperfusion injury increased the content of paeoniflorin, calycosin, calycosin-7-o- β -d-6-glucoside, and 6-gingerol in the blood, affecting the clearance rate of paeoniflorin in the brain, the detention time of calycosin-7-o- β -d-6-glucoside and the 6-gingerol in the brain. In normal and cerebral ischemia-reperfusion rats, the content of paeoniflorin and 6-gingerol in the blood was higher than that in brain tissue, while the content of calycosin, calycosin-7-o- β -d-6-glucoside in the brain tissue was higher than that in blood, suggesting that calycosin and calycosin-7-o- β -d-6-glucoside have brain targeting properties.

Keywords: Huangqi Guizhi Wuwu Decoction, microdialysis, paeoniflorin, calycosin-7-o- β -d-6-glucoside, calycosin, 6-gingerol, pharmacokinetics

Introduction

Stroke is severely detrimental to human health, with ischemic stroke accounting for the largest proportion of all strokes (about 85%).¹ Approximately three-fourths of surviving patients present different degrees of dysfunction,^{2,3} which seriously affects the patients' quality of life and increases the burden on families and society.

Correspondence: Li-Sheng Wang
Tel +86 20-39358290
Email wlis68@126.com

Currently, the main treatment strategy for ischemic stroke is thrombolytic therapy, however, its rate of utilization is low due to the limited time window and other complications. Several neuroprotective agents are available including edaravone, calcium antagonist, cytosolic choline, etc. However, their efficacy and long-term effects need to be further investigated.

Huangqi Guizhi Wuwu Decoction (HGWD) has been derived from the “Jinyi Yaoluo, Blood Stasis, and Diseases”, and includes five herbs namely *Astragali*, *Ramulus Cinnamomi*, *Paeoniae Radix Alba*, *Zingiberis Rhizoma Recens*, *Jujubae Fructus* for the treatment of blood stasis. Interestingly, modern clinical applications have surpassed the original prescription for the treatment of “blood stasis” and have achieved satisfactory results. Clinical research has indicated that HGWD can significantly improve neurological and motor functions in patients recovering from a stroke, improving the self-care ability and treating shoulder-hand syndrome after stroke.^{4–6}

Calycosin-7-O- β -D-6-glucoside (CG) and calycosin (CA) are two representative flavonoids present in *Astragalus*.⁷ Studies have demonstrated that CG can inhibit the mitochondrial membrane potential (MMP) activation, protect the blood-brain barrier, reduce cerebral infarction volume,^{8,9} activate PI3K/Akt pathway, and play a neuroprotective role in cerebral ischemia-reperfusion injury.¹⁰ Paeoniflorin (PF) has demonstrated the ability to scavenge free radicals in cell or non-cellular systems, inhibit the biological activity of MMP-9,^{11–13} inhibit the production of ROS, preserve the cytoskeletal structure to attenuate the permeability of human umbilical vein endothelial cells (HUVECs) under hypoxic conditions,¹⁴ prevent calcium overload as a non-competitive calcium channel blocker,¹⁵ regulate positive feedback of estrogen receptor ER- α and microRNA-375 during cerebral ischemia-reperfusion injury.¹⁶ PF is a mono- β -glycoside isolated from *Paeoniae Radix Alba* and is also the main active ingredient of ferrets. Studies have shown that PF has a neuroprotective role in cerebral ischemia-reperfusion models, both in vivo¹⁷ and in vitro, induced by H₂O₂,¹⁸ MPP⁺,¹⁹ 6-glutamate,²⁰ A β 25–35,²¹ and lipopolysaccharide.²² Furthermore, studies have demonstrated that PF may regulate cerebral ischemia-reperfusion injury by regulating the Ca²⁺/CaMKII/CREB signaling pathway.²³ The main chemical components in *Zingiberis Rhizoma Recens* are 6-Gingerol (6-G) and flavonoids. Wattanathorn et al²⁴ observed that in rats

administered the root extract of *Zingiberis Rhizoma Recens*, the cognitive function and hippocampal neuron density improved and the volume of cerebral infarction decreased. Na et al²⁵ reported that aqueous *Zingiberis Rhizoma Recens* extract has protective effects in cerebral ischemia and ischemia-reperfusion injury. This mechanism may be related to reduced expression of caspase-3 and increased ratio of Bcl-2/Bax in MCAO rats.

Pharmacokinetic study plays an important role in clinical applications with regard to determination of the clinical dose and avoiding side effects. In the early stage, our research group detected CG, CA, PF and 6-G in the blood and brain of HGWD in rats. The present study was first carried out using microdialysis technique to investigate pharmacokinetic differences of these blood-entering active ingredients in normal and cerebral ischemic injury rats after oral administration of HGWD. The pharmacokinetics behavior results of CG, CA, PF and 6-G enable a better understanding of the complex mechanisms of absorption, distribution, metabolism, excretion and safety for future clinical applications; also partly clarifying the rationality and compatibility of the prescriptions containing *Astragalus*, *Paeoniae Radix Alba* and *Zingiberis Rhizoma Recens*.

Experimental Methods and Materials

Chemicals and Reagents

CA, PF, CG, and 6-G standards were purchased from Chengdu Pfeiffer Biotechnology Co., Ltd (China), which complies with the 2015 edition of the Chinese Pharmacopoeia. In addition, they were identified as authentic by Professor Zhang Danyan of Guangzhou University of Chinese Medicine and were stored at 4 °C. Sulfamethoxazole (internal standard, IS; 99.5 % purity) was purchased from Aladdin Chemistry Co., Ltd (Shanghai, China). HPLC grade acetonitrile, methanol, and formic acid were procured from Thermo Fisher Company Inc. (Waltham, MA, USA). Ulatan was obtained from Shanghai Sinopharm Chemical Reagent Co., Ltd (China). Sodium chloride, potassium chloride, anhydrous calcium chloride, and magnesium chloride were provided by the Guangzhou Chemical Reagent Factory (Guangzhou, China) and identified by Professor Danyan Zhang of the Guangzhou University of Chinese Medicine (Guangzhou, China). Triple deionized water from

Millipore (Bedford, MA, USA) was used to prepare all aqueous solutions.

Preparation of HGWD

The herbs of *Radix Astragali* (1296 g), *Ramulus Cinnamomi* (1296 g), *Paeoniae Radix Alba* (1296 g), *Zingiberis Rhizoma Recens* (2592 g), *Jujubae Fructus* (1296 g) were purchased from the Guangzhou Zhixin Chinese Herbal Pieces Co., Ltd (180,402–180,602), which complies with the 2015 Chinese Pharmacopoeia. Herbs were certified as authentic by Professor Danyan Zhang from Guangzhou University of Chinese Medicine. The herbal admixture was soaked in water for 30 min and was thrice decocted in a water bath for 3 h. The least volume of solvent was added to the 85% ethanol, and refrigerated for 24 h. Under suction filtration, the ethanol filtrate was recovered under reduced pressure to a non-alcoholic taste. The filtrate was concentrated to a small volume and then placed in a 100 mL volumetric flask. The volume was adjusted to a volume of 6.48 g·mL⁻¹ of HGWD.

Animals

Sprague Dawley SPF male rats (270–300 g) were provided by the Experimental Animal Center of the Guangzhou University of Traditional Chinese Medicine. (approval number: SCXK Yue 2013–0034). All experiments were performed in accordance with the NIH guidelines and approved by the Animal Care and Use Committee of the Guangzhou University of Chinese Medicine (Guangdong, China). In the first experiment, rats (n=12) were utilized to establish the HPLC-MS/MS methodology and pharmacokinetics study. All rats were randomly divided into two groups: group 1 (Control group) was treated with HGWD (48.6 g·Kg⁻¹, intragastric administration); group 2 (MCAO group) was treated with HGWD (48.6 g·Kg⁻¹, intragastric administration).

The middle cerebral artery occlusion (MCAO) model was established according to the method of Longa with minor modifications.²⁶ The rats were anesthesia using 10% chloral hydrate (3–3.0 mL·kg⁻¹) via intraperitoneal injection. After disinfection of the neck region, the right common carotid artery (CCA), the external carotid artery (ECA), and the internal carotid artery (ICA) were isolated, and the ECA and CCA were ligated. A 0.26-mm polylysine-coated nylon monofilament was inserted through the ICA to occlude the middle cerebral artery (MCA) in the brain. After the rats were ischemic for 2 h, the suture was pulled back by about 10 mm. The suture was removed, with reperfusion performed for 22 h.

Liquid Chromatography and Mass Spectrometric Conditions

Chromatographic conditions: Phenomenex Kinetex C18 column (50 × 2.1 mm, 2.6 μm); mobile phase: 0.05% formic acid water (A) - acetonitrile (B), flow rate 200 μL·min⁻¹, injection volume 5 μL, column temperature 35 °C; mobile phase gradient elution procedure: 0–2 min (90–70% A), 2–4.5 min (70–60% A), 4.5–7 min (60–50% A), 9–10 min (40–10% A).

Mass spectrometry conditions: electrospray ionization (ESI) positive ion mode scan, capillary voltage: 4500 V; dryer temperature: 300 °C; dryer flow rate: 5 L·min⁻¹; sheath gas temperature: 250 °C; sheath gas flow rate: 11 L·min⁻¹; nebulizer gas pressure: 45 psi; nozzle voltage: 500 V. Ion detection method: The multiple reaction monitoring (MRM) mode was selected, the PF ion pair was m/z [M+NH₄]⁺+498.20→179.01 (CE:17V), CG ion pair was m/z [M+H]⁺+447.2→285.1 (CE: 15 V), IS daughter ion pair was m/z [M+H]⁺+254.15→156.05 (CE:13 V), CA ion pair was m/z [M+H]⁺+285.2→270.2 (CE: 25 V), the 6-G parent ion pair was m/z [M+H]⁺+312→137.2 (CE: 33 V). The structural formulas of PF, CG, CA, 6-G and sulfamethoxazole are as shown in Figure 1.

Preparation of Calibration Standards and Quality Control Samples (QC)

The mixed stock standard solution was prepared in methanol containing CA (5 μg·mL⁻¹), PF (5 μg·mL⁻¹), CG (5 μg·mL⁻¹), and 6-G (μg·mL⁻¹). IS was prepared at a concentration of 604 ng·mL⁻¹ in methanol. The working solutions were further diluted with artificial cerebrospinal fluid (ACSF solutions) and blank Ringer's solution (BRS) to the appropriate daily concentrations. Prior to each analytical run, the calibration standards (30 μL) were critically extracted in EP tubes and the solvent was vacuum evaporated using 30 μL of the mobile phase to dissolve each calibration standard. The QC samples were obtained at the following concentrations: CA (800 μg·mL⁻¹), PF (1200 μg·mL⁻¹), CG (458 μg·mL⁻¹) and 6-G (942 μg·mL⁻¹). All solutions were stored at -4 °C prior to use.

Method Validation

Specificity

The specificity of the method was established by analyzing the blank brain microdialysis samples obtained from six different rats. The potential interference of endogenous dialysate matrix components was investigated at the retention

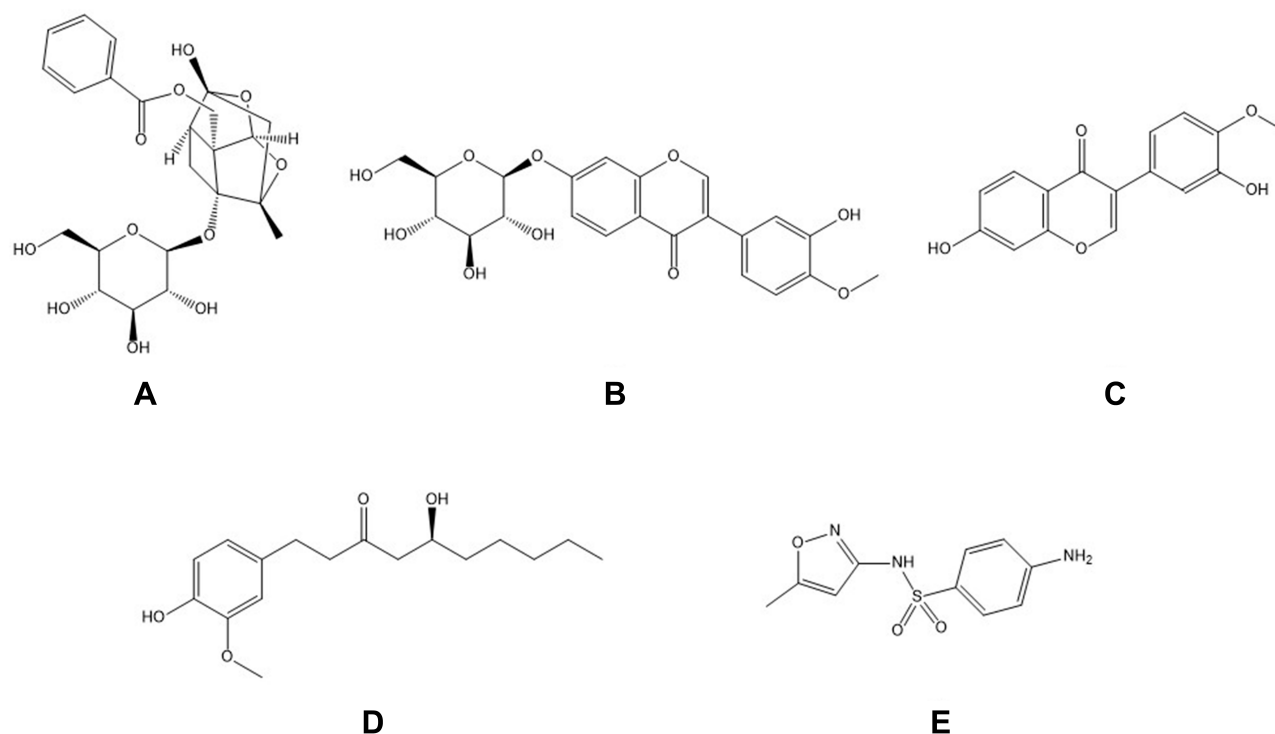


Figure 1 The structure of the object to be tested and the internal standard (A) paeoniflorin; (B) calycosin-7-O-β-D-glucoside; (C) calycosin; (D) 6-gingerol; (E) sulfamethoxazole.

times of all analytes and IS by analyzing the response of the blank dialysate, blank dialysate spiked with IS at LLOQ and dialysate samples obtained 2 h after administration.²⁷

Linearity and LLOQ

The linearity of the method was evaluated by testing each concentration level of the seven calibration standards in duplicate over three consecutive days. The calibration curves were constructed by plotting the peak area ratios (y) of the analyte to IS versus the nominal concentrations of the analyte (x) by weighted ($1/x^2$) least-square linear regression. The LLOQ was defined as the lowest concentration of the calibration curve producing a signal-to-noise ratio (S/N) >10 . The LLOQ was measured by using six independent standards and determining the coefficient of variation (CV). An acceptable CV should be within 20%.

Precision Test

Precision was determined by analyzing six replicate concentrations of QC samples within 24 h. The value of accuracy and precision was required to be within $\pm 15\%$.

Matrix Effect

The matrix effects for CA, PF, CG, 6-G, and IS were assessed by assaying six replicates of QCs at three concentration levels.

This was assessed by comparing the peak area of CA, PF, CG, 6-G, and IS in the blank dialysate with the same concentrations of CA, PF, CG, 6-G and IS in the mobile phase.

Stability

The stability of CA, PF, CG, 6-G, and IS was evaluated by analyzing QCs at three concentration levels under different conditions. These QCs were analyzed after storage at room temperature for 8 h (benchtop stability), at -70°C for 30 days (long term stability), after three freeze-thaw cycles at -70°C and at 4°C for 24 h (autosampler stability).

Microdialysis Experiments

The microdialysis system (CMA, Stockholm, Sweden) consisted of a microinjection pump (CMA/402, Stockholm, Sweden) and microsyringe (MS-GAN100, Stockholm, Sweden). Following anesthesia under urethane, the rats were fixed using a stereotaxic instrument, and a cannula with a stylet was implanted in the left striatum (A: $+0.2$ mm; L: 3.2 mm; H: $+3.0$ mm). A hole was drilled in the skull and at a position in triangulation with the cannula implantation position, the screw was implanted, and the sleeve was fixed with the dental powder. After the cement was indurated, the rat's ventral surface faced upwards, the jugular vein was bluntly separated and the distal end was

ligated. A small opening was made at the distal end using ophthalmic scissors, and a blood probe was implanted at about 2.5 cm. After the blood probe was implanted, the rat was placed in the prone position, the stylet was pulled out, and the brain probe was implanted.

After probe implantation, the drug-containing ACSF and Ringer's solution (the concentration of CA, PF, CG, and the 6-G was $5 \mu\text{g}\cdot\text{mL}^{-1}$) were equilibrated at a flow rate of $1.5 \mu\text{L}\cdot\text{min}^{-1}$. After 1 h, three microdialysis fluids (C_{dialysis}) with a volume of $30 \mu\text{L}$ were obtained, and the concentration of the medicinal perfusate was recorded as ($C_{\text{perfusate}}$). After 2.5 h in vivo, the samples were collected 2 min after administration. A sample was collected at intervals of 10 min between 5 and 55 min, and one sample was collected every 20 min until 415 min. The collected samples were stored in a $-20 \text{ }^{\circ}\text{C}$ refrigerator for further processing.

Before the probe was implanted, the probe was placed in a heparin sodium injection and perfused with blank Ringer's solution and blank ACSF at a perfusion rate of $1.5 \mu\text{L}\cdot\text{min}^{-1}$ for 30 min. All samples collected at intervals of 10 min were added with $15 \mu\text{L}$ of corresponding blank perfusion solution. All microdialysis samples were added with $10 \mu\text{L}$ sulfamethoxazole (604 ng/mL), vortexed for 4 min. Next, the flow injection analysis was performed, and the peak area recorded. The drug concentration was calculated and the relative loss rate (RL) in the body was calculated from the formula (1), and the actual concentration of the drug was calculated by the formula $C_{\text{actual}} = C_{\text{Measured}}/\text{RL}$.

$$RL = (C_{\text{perfusate}} - C_{\text{dialysis}}) / C_{\text{perfusate}} \times 100\% \quad (1)$$

Statistical Analysis

All data are presented as mean \pm standard deviation (SD). The statistical significance was analyzed by the Student's unpaired *t*-test using SPSS Version 17.0 (IBM Corporation, Armonk, NY, USA). $P < 0.05$ was considered statistically significant. The pharmacokinetic parameters of PF, CG, CA, and 6-G were analyzed using PKSolver²⁸ (version 2.0; China Pharmaceutical University, Nanjing, China) by the noncompartmental analysis.

Results and Discussion

Method Validation

Specificity

The blank blood and brain microdialysis solutions before administration, the blood and brain microdialysis samples

after administration, and the standard mixture solution. Each $30 \mu\text{L}$, except for the blank dialysate, were obtained and $10 \mu\text{L}$ of the IS was added; Next, the samples were vortexed for 4 min and analyzed using UPLC-MS/MS. As shown in Figure 2, the peak shape of the analyte and the IS in the reference solution and the microdialysis sample are symmetric, the retention time of PF, CG, CA, 6-G, and IS were 4.07, 4.67, 6.17, 8.71, and 5.10 min.

Linearity and LLOQ

The results demonstrated that the linear regression equations for PF, CG, CA, and the 6-G in blood microdialysis solution were: $Y = 3 \times 10^{-5} X - 4 \times 10^{-4}$ (0.9996), linear range $45\text{--}1200 \text{ ng}\cdot\text{mL}^{-1}$; $Y = 2 \times 10^{-5} X - 5 \times 10^{-5}$ (0.9993), linear range was $15\text{--}1200 \text{ ng}\cdot\text{mL}^{-1}$; $Y = 1 \times 10^{-4} X - 1 \times 10^{-4}$ (0.9997). The linear range was $20\text{--}1200 \text{ ng}\cdot\text{mL}^{-1}$; $Y = 6 \times 10^{-6} X - 8 \times 10^{-5}$ (0.9975), and the linear range was $100\text{--}1000 \text{ ng}\cdot\text{mL}^{-1}$.

The linear regression equations for PF, CG, CA, and 6-G in the brain microdialysis solution were: $Y = 3 \times 10^{-5} X - 4 \times 10^{-4}$ (0.9979), the linear range was $15\text{--}1200 \text{ ng}\cdot\text{mL}^{-1}$; $Y = 2 \times 10^{-5} X - 4 \times 10^{-5}$ (0.9992), linear range was $15\text{--}1200 \text{ ng}\cdot\text{mL}^{-1}$; $Y = 2 \times 10^{-4} X - 2 \times 10^{-4}$ (0.9973), linear range was $100\text{--}2000 \text{ ng}\cdot\text{mL}^{-1}$ and $Y = 2 \times 10^{-5} X + 2 \times 10^{-4}$ (0.9993), the linear range was $100\text{--}2000 \text{ ng}\cdot\text{mL}^{-1}$. The LLOQ ($S/N > 10$) of the analytes were: $3.73 \text{ ng}\cdot\text{mL}^{-1}$ for PF, $2.78 \text{ ng}\cdot\text{mL}^{-1}$ for CG, $18.24 \text{ ng}\cdot\text{mL}^{-1}$ for CA and $35.88 \text{ ng}\cdot\text{mL}^{-1}$ for 6-G in the brain and blood microdialysis solution.

Precision Test

Here, the low, medium, and high concentrations of PF, CG, CA, and 6-G solution ($15/15/100/100$; $105/105/1200/1200$; $1500/1500/1600/1600 \text{ ng}\cdot\text{mL}^{-1}$) were continuously injected six times and the peak areas were recorded. The results are as shown in Table 1.

Matrix Effect

A: The PF/CG/CA/6-G reference solution was added to the blank brain or blood microdialysis solution and formulated into low, medium and high concentration ($15/15/100/100$; $105/105/1200/1200$; $1500/1500/1600/1600 \text{ ng}\cdot\text{mL}^{-1}$) solutions. Next, the injection was repeated three times and the peak area A was recorded.

B: The PF/CG/CA/6-G reference solution was added to the ACSF and Ringer's solution and formulated into low, medium, and high concentration ($15/15/100/100$; $105/105/1200/1200$; $1500/1500/1600/1600 \text{ ng}\cdot\text{mL}^{-1}$) sample solutions. The injection was three times and

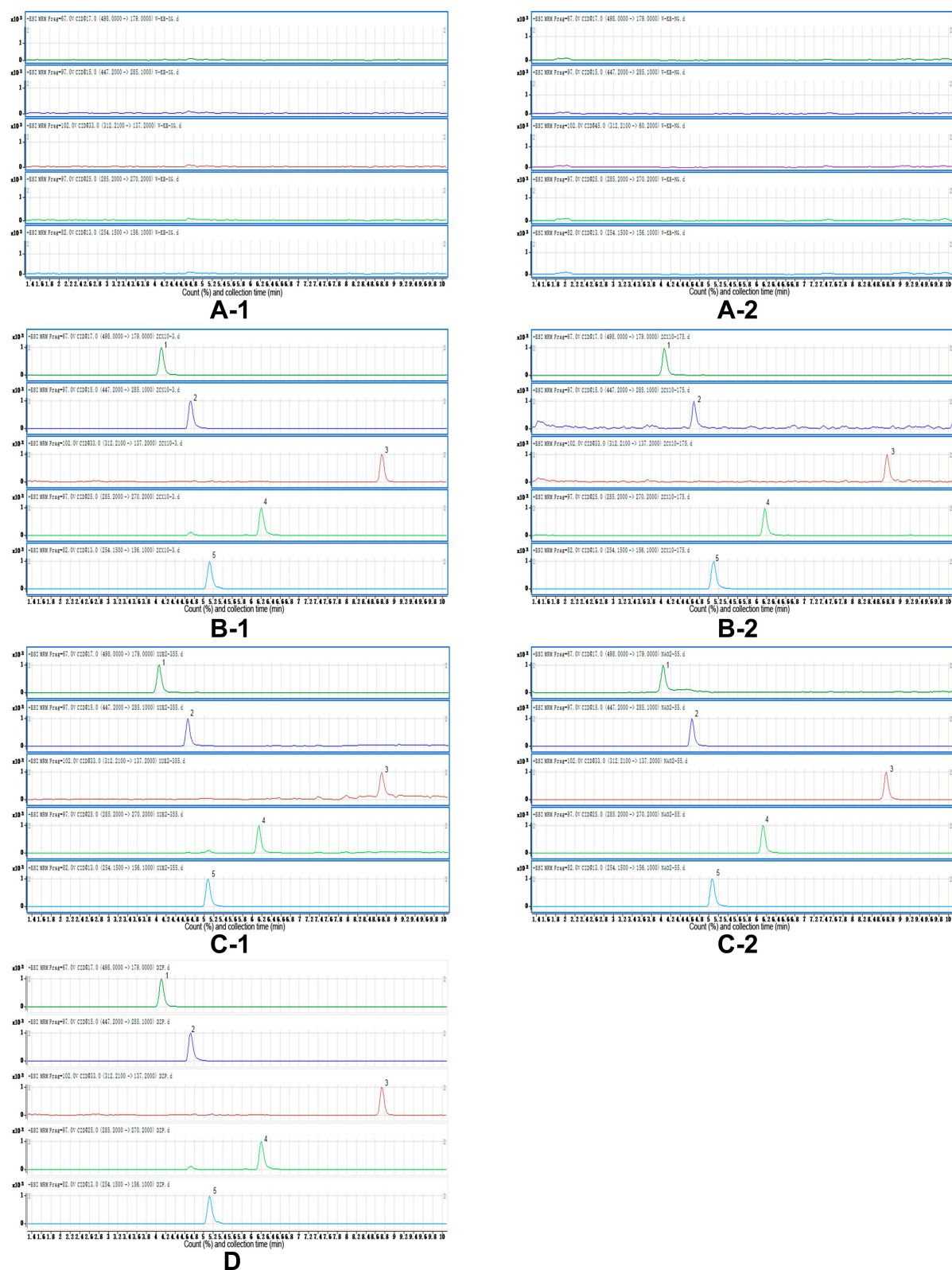


Figure 2 HPLC-MS/MS diagram (**A-1**): blank blood microdialysis solution; (**B-1**): normal rat blood microdialysis solution sample + internal standard; (**C-1**): model rat blood microdialysis solution sample + internal standard; (**A-2**): blank brain microdialysis solution; (**B-2**): normal rat brain microdialysis solution sample + internal standard; (**C-2**): model rat brain microdialysis solution sample + internal standard; (**D**) control product + internal standard. 1: paeoniflorin; 2: calycosin-7-O- β -D-glucoside; 3: calycosin; 4: 6-gingerol; 5: sulfamethoxazole).

Table 1 The Results of the Precision Investigation of Paeoniflorin, Calycosin-7-O- β -D-6-Glucoside, Calycosin, and 6-Gingerol

C (ng/mL)		1	2	3	4	5	6	RSD(%)
PF	15	1945	1985	2100	1957	1964	2171	4.60
	105	11,253	11,268	10,805	11,308	11,595	10,190	4.52
	1500	150,646	148,450	150,689	151,915	142,514	148,122	2.27
CG	15	42,974	43,498	42,122	41,109	39,747	40,527	3.49
	105	228,504	237,535	220,671	243,369	223,245	229,638	3.73
	1500	2,249,986	2,156,205	2,239,179	2,231,842	2,227,542	2,195,645	1.57
CA	100	37,942	35,695	36,887	35,780	35,778	36,158	2.44
	1200	261,904	259,859	269,968	245,584	269,218	282,936	4.71
	1600	374,661	365,461	361,585	333,200	369,988	352,422	4.17
6-G	100	3924	3881	3964	3957	4218	3882	3.18
	1200	46,086	44,001	45,356	46,170	45,661	43,876	2.25
	1600	63,196	64,002	65,336	70,472	62,584	63,644	4.46

the peak area B was recorded. The matrix effect was calculated using A/B. The results are as shown in Table 2.

Table 2 Results of the Matrix Effect

		C(ng/mL)	A	B	A/B (%)
BRS solution	PF	15	2454	2621	93.62
		105	10,568	11,084	95.34
		1500	177,465	175,364	101.20
	CG	15	30,279	30,549	99.12
		105	178,034	176,781	100.71
		1500	2,521,251	2,516,766	100.18
	CA	100	35,203	33,545	104.95
		1200	253,290	253,920	99.75
		1600	661,957	665,743	99.43
	6-G	100	3437	3450	99.60
		1200	49,746	48,931	101.66
		1600	62,268	63,363	98.27
ACSF solution	PF	15	3365	3541	95.02
		105	11,962	11,967	99.96
		1500	179,604	183,836	97.70
	CG	15	31,623	32,031	98.73
		105	175,211	184,710	94.85
		1500	2,522,758	2,640,361	95.55
	CA	100	35,931	36,014	99.77
		1200	256,858	257,310	99.82
		1600	664,978	662,009	100.45
	6-G	100	3660	3675	99.58
		1200	41,171	46,658	88.24
		1600	62,584	65,215	95.96

Stability

The low, medium, and high concentrations of the PF, CG, CA, and 6-G reference solutions (15/15/100/100; 105/105/1200/1200; 1500/1500/1600/1600 ng·mL⁻¹) were injected at 0, 4, 6, 8, 12, and 24 h, and the peak areas were recorded. The results are as shown in Table 3.

Pharmacokinetic Profiles

The blood and brain tissue samples obtained from the rats to which had been administrated by gavage were determined by the HPLC-MS/MS method. The plasma concentration–time curves of PF, CG, CC, and 6-G in the blood of normal rats and model rats are shown in Figure 3. The plasma concentration–time curves of PF, CG, CA, and 6-G in brain tissues of rats with cerebral ischemic injury are shown in Figure 4. The main brain pharmacokinetic parameters of PF, CG, CA, and 6-G in plasma and brain tissue samples of normal rats and model rats were summarized and listed in Tables 4–7 by statistical moment method. The results showed that PF, CG, CA, and 6-G were detected in the rat blood and brain tissue samples 5 min after ig administration, demonstrating the target compounds were capable of permeating the BBB. The good BBB permeability was probably related to their small molecular weight and the protein binding rate.

As can be seen from Table 4, compared with normal group, the dose-dependent maximum concentration (C_{max}) of drug and the area under the curve from 0 to 415 min ($AUC_{0\rightarrow t}$) in the blood of PF were significantly increased, the clearance rate (CL_{blood}) in the blood, the half-life ($t_{1/2}$) and the apparent volume of distribution in the brain tissue (V_{brain}) decreased in model group following the

Table 3 The stability Results of Paeoniflorin, Calycosin-7-O- β -D-6-Glucoside, Calycosin, and 6-Gingerol

	C (ng/mL)	0h	4h	6h	8h	12h	24h	RSD (%)
PF	15	1069	1161	1121	1114	1182	1208	4.44
	105	9194	8759	8564	8766	8407	8317	3.64
	1500	149,457	156,344	145,498	154,465	147,269	142,613	3.54
CG	15	30,492	30,217	31,060	31,184	29,302	30,695	2.24
	105	208,794	227,669	222,692	216,448	236,903	231,521	4.58
	1500	2,216,623	2,316,097	2,216,728	2,224,813	2,205,025	221,367	1.86
CA	100	32,377	33,411	34,000	34,053	33,523	333,646	1.81
	1200	263,518	264,814	266,626	268,467	258,172	256,155	1.84
	1600	368,938	339,928	372,843	339,489	372,263	361,500	4.34
6-G	100	4390	4675	4407	4460	4489	4564	2.38
	1200	43,474	45,445	47,261	44,113	44,605	46,530	3.22
	1600	65,638	64,437	67,295	65,985	67,076	66,966	1.66

administration of HGWD, indicating that cerebral ischemia-reperfusion injury may affect the permeability of blood-brain barrier (BBB) and affect the metabolism of PF in the brain.

As can be seen from Tables 5 and 6, the rats in the model group demonstrated lower levels of $C_{\max \text{ blood}}$, $AUC_{0-t \text{ blood}}$, $AUC_{0-\infty \text{ blood}}$, and MRT_{brain} and higher

levels of CL_{blood} and $C_{\max \text{ brain}}$ of CG compared to control group following the administration of HGWD, compared to the rats in the normal group, the $C_{\max \text{ blood}}$ was decreased, V_{blood} and V_{brain} of the CA were increased in model rats following the administration of HGWD. According to literature reports,²⁹ after intragastric administration of CA suspension (administration

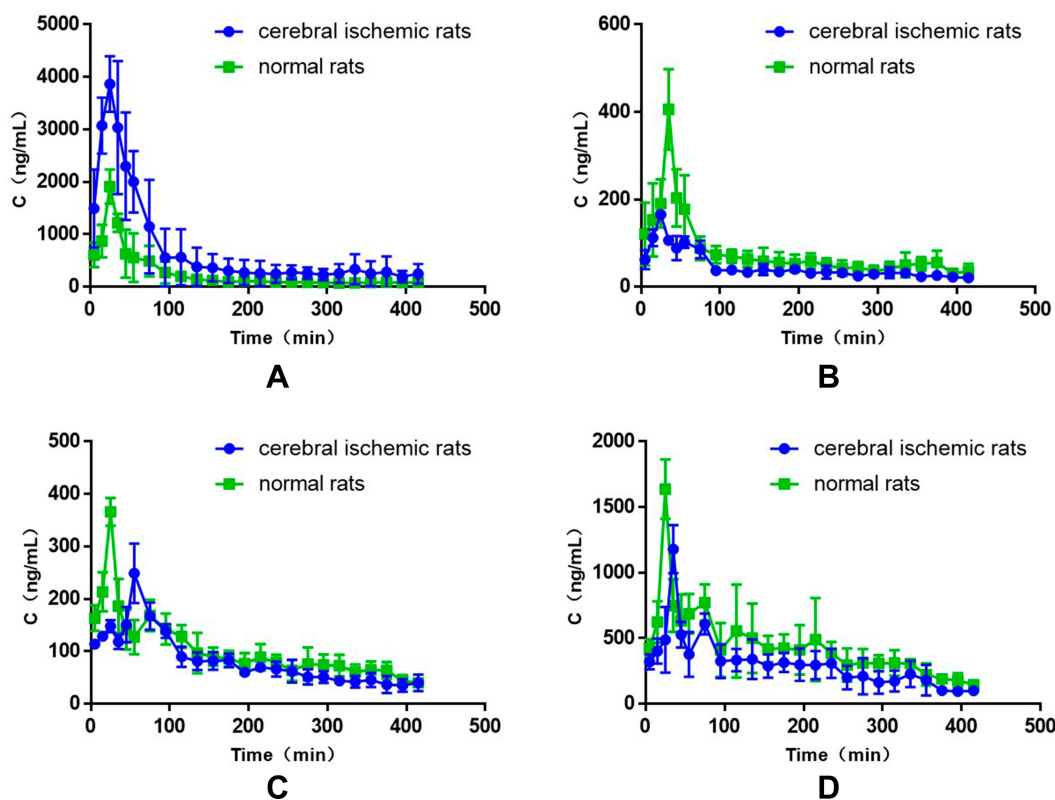


Figure 3 The drug-time curve of each components in blood of normal rats and cerebral ischemic rats (A): paeoniflorin; (B) calycosin-7-O- β -D-6-glucoside; (C) calycosin; (D) 6-gingerol.

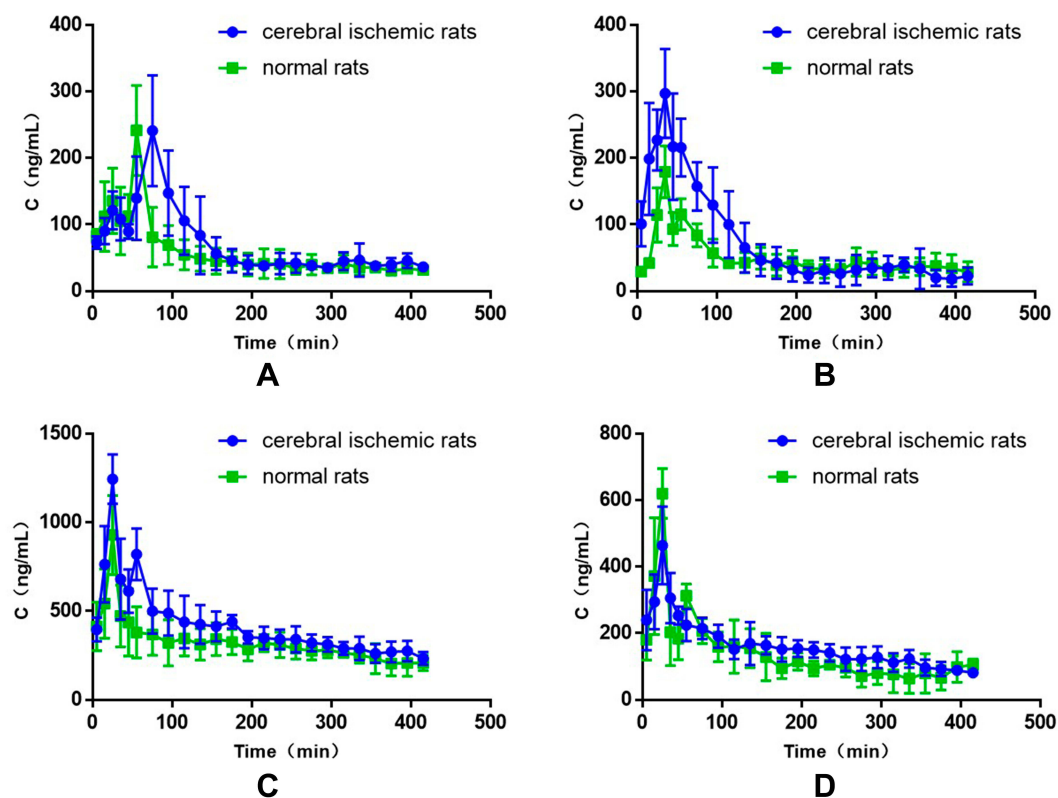


Figure 4 The drug-time curve of each components in brain tissue of normal rats and cerebral ischemic rats (A): paeoniflorin; (B) calycosin-7-O- β -D-6-glucoside; (C) calycosin; (D) 6-gingerol.

dose of 120 mg/kg), it was found that the plasma concentration–time curves of CA was double-peaked in the portal vein and systemic plasma, and the first peak time (T_{max}) appeared at 0.5 h or 1 h, the second T_{max} appears at 4 h, and in this experiment, there is also a double peak in the plasma concentration–time curves of CA of the blood and brain tissues, the first T_{max} appears around at 25 min, and the second T_{max} appeared at about 55 min, indicating that the first T_{max} of CA is

due to the absorption of CA contained in the drug, and the second T_{max} may be the formation of CA after the deglycosylation of CG in the intestine and intestinal cells. Studies have shown that the drug concentration of CA in tissues is higher than that of systemic plasma, and the drug concentration in liver, kidney and heart is 212.1, 30.5 and 4.7 times that of systemic plasma.²⁹ The results of this experiment showed that the drug concentration of CA in normal rat brain tissue is about 2.54

Table 4 The Pharmacokinetic Parameters of Paeoniflorin (PF) After the Intra-gastric Administration of Huangqi Guizhi Wuwu Decoction (HGWD) (Mean \pm SD, n=5)

parameters	Blood		Brain	
	Normal Group	Model Group	Normal Group	Model Group
$t_{1/2}$ (min)	118.16 \pm 71.06	96.75 \pm 10.22	256.96 \pm 66.80	168.67 \pm 67.09*
T_{max} (min)	25.00 \pm 0.00	27.00 \pm 4.47	55 \pm 0.00	70.00 \pm 10.00
C_{max} (ng/mL)	1909.06 \pm 327.89	4213.90 \pm 312.58*	241.01 \pm 67.97	259.62 \pm 62.01
V(L/g)	0.72 $\times 10^{-1}$ \pm 0.05 $\times 10^{-1}$	0.24 $\times 10^{-1}$ \pm 0.94 $\times 10^{-2}$	0.50 \pm 0.13	0.29 \pm 0.88 $\times 10^{-1}$ *
CL(L/min/g)	0.41 $\times 10^{-3}$ \pm 0.73 $\times 10^{-4}$	0.17 $\times 10^{-3}$ \pm 0.65 $\times 10^{-4}$ *	0.14 $\times 10^{-2}$ \pm 0.20 $\times 10^{-3}$	0.13 $\times 10^{-1}$ \pm 0.16 $\times 10^{-3}$
AUC _{0-t} (ng \cdot min/mL)	105,602.50 \pm 30,163.61	28,992.70 \pm 9887.48*	24,153.66 \pm 6022.95	29,630.79 \pm 5406.79
AUC _{0-inf} (ng \cdot min/mL)	120,865.95 \pm 23,807.93	323,128.70 \pm 120,169.60*	36,126.75 \pm 4889.72	37,282.84 \pm 4937.62
MRT(min)	118.16 \pm 71.06	141.82 \pm 38.14	369.68 \pm 117.26	253.22 \pm 33.08

Note: Compared to the normal group, *p<0.05.

Table 5 The Pharmacokinetic Parameters of Calycosin-7-O- β -D-6-Glucoside (CG) After the Intragastric Administration of Huangqi Guizhi Wuwu Decoction (HGWD) (Mean \pm SD, n=5)

Parameters	Blood		Brain	
	Normal Group	Model Group	Normal Group	Model Group
$t_{1/2}$ (min)	118.88 \pm 73.69	67.02 \pm 22.15	136.08 \pm 48.17	100.51 \pm 27.38
T_{max} (min)	35.00	25.00	25.00	35.00
C_{max} (ng/mL)	405.72 \pm 91.83	164.62 \pm 14.37*	179.31 \pm 39.18	296.76 \pm 66.77*
V(L/g)	0.21 \pm 0.12	0.21 \pm 0.49 $\times 10^{-1}$	0.37 \pm 0.15	0.21 \pm 0.40 $\times 10^{-1}$
CL(L/min/g)	0.13 $\times 10^{-2}$ \pm 0.33 $\times 10^{-3}$	0.22 $\times 10^{-2}$ \pm 0.24 $\times 10^{-3}$ *	0.19 $\times 10^{-2}$ \pm 0.25 $\times 10^{-3}$	0.15 $\times 10^{-2}$ \pm 0.45 $\times 10^{-3}$
AUC _{0-t} (ng \cdot min/mL)	31,989.03 \pm 5567.43	19,765.76 \pm 1303.65*	20,793.80 \pm 2278.58	30,892.47 \pm 10,160.71
AUC _{0-inf} (ng \cdot min/mL)	38,955.92 \pm 10,414.34	21,797.11 \pm 2322.96*	26,235.78 \pm 3986.80	34,529.29 \pm 12,908.44
MRT (min)	223.54 \pm 77.90	185.63 \pm 25.17	256.15 \pm 44.13	157.94 \pm 34.94*

Note: Compared to the normal group, *p<0.05.

Table 6 The Pharmacokinetic Parameters of the Calycosin (CA) After the Intragastric Administration of Huangqi Guizhi Wuwu Decoction (HGWD) (Mean \pm SD, n=5)

Parameters	Blood		Brain	
	Normal Group	Model Group	Normal Group	Model Group
$t_{1/2}$ (min)	114.91 \pm 70.41	184.87 \pm 30.19	341.06 \pm 33.77	301.87 \pm 84.55
T_{max} (min)	25.00	55.00	25.00	25.00
C_{max} (ng/mL)	366.20 \pm 26.72	249.04 \pm 56.82*	928.52 \pm 223.33	1243.06 \pm 139.00
V(L/g)	0.16 \pm 0.85 $\times 10^{-1}$	0.28 \pm 0.81 $\times 10^{-2}$ *	0.10 \pm 0.19 $\times 10^{-1}$	0.76 $\times 10^{-1}$ \pm 0.59 $\times 10^{-2}$ *
CL(L/min/g)	0.10 $\times 10^{-2}$ \pm 0.17 $\times 10^{-3}$	0.11 $\times 10^{-2}$ \pm 0.21 $\times 10^{-3}$	0.21 $\times 10^{-3}$ \pm 0.49 $\times 10^{-4}$	0.18 $\times 10^{-3}$ \pm 0.29 $\times 10^{-4}$
AUC _{0-t} (ng \cdot min/mL)	42,207.43 \pm 5419.50	34,611.25 \pm 2837.95	133,272.60 \pm 32,388.54	172,537.00 \pm 11,809.28
AUC _{0-inf} (ng \cdot min/mL)	49,022.41 \pm 7180.82	45,800.72 \pm 8677.20	236,782.00 \pm 62,690.52	277,235.10 \pm 53,781.61
MRT(min)	219.33 \pm 49.12	275.74 \pm 66.18	495.49 \pm 24.57	424.45 \pm 118.84

Note: Compared to the normal group, *p<0.05.

Table 7 The Pharmacokinetic Parameters of 6-Gingerol (6-G) After the Intragastric Administration of Huangqi Guizhi Wuwu Decoction (HGWD) (Mean \pm SD, n=5)

Parameters	Blood		Brain	
	Normal Group	Model Group	Normal Group	Model Group
$t_{1/2}$ (min)	81.53 \pm 21.68	111.81 \pm 58.82	200.14 \pm 41.05	203.43 \pm 38.11
T_{max} (min)	25.00	35.00	25.00	25.00
C_{max} (ng/mL)	1638.33 \pm 226.86	1179.01 \pm 183.50*	619.39 \pm 75.06	506.44 \pm 98.18
V(L/g)	0.29 $\times 10^{-1}$ \pm 0.74 $\times 10^{-2}$	0.57 $\times 10^{-1}$ \pm 0.31 $\times 10^{-1}$	0.16 \pm 0.12 $\times 10^{-1}$	0.16 \pm 0.24 $\times 10^{-1}$
CL(L/min/g)	0.25 $\times 10^{-3}$ \pm 0.29 $\times 10^{-4}$	0.35 $\times 10^{-3}$ \pm 0.62 $\times 10^{-4}$ *	0.57 $\times 10^{-3}$ \pm 0.11 $\times 10^{-3}$	0.54 $\times 10^{-3}$ \pm 0.54 $\times 10^{-4}$
AUC _{0-t} (ng \cdot min/mL)	181,512.7 \pm 21,224.04	124,603.40 \pm 24,478.73*	57,807.41 \pm 16,179.63	65,362.58 \pm 8471.59
AUC _{0-inf} (ng \cdot min/mL)	199,404.60 \pm 25,065.61	141,867.60 \pm 22,157.00*	87,520.56 \pm 19,259.47	90,045.81 \pm 9498.28
MRT(min)	191.52 \pm 12.45	210.69 \pm 30.77	338.28 \pm 6.73	313.97 \pm 10.36*

Note: Compared to the normal group, *p<0.05.

times that in blood, while the drug concentration of CA in brain tissue of model rats is about 4.98 times that in blood, suggesting that CA can be used in the treatment of brain diseases, and cerebral ischemia-reperfusion injury can increase the distribution of CA in brain tissue.

As can be seen from Table 7, compared to the normal group, the 6-G C_{max} blood, AUC_{0-t} blood, AUC_{0-inf} blood, and MRT_{brain} were all decreased, and CL_{blood} of the 6-G was increased in the rats in the model group following the administration of HGWD, indicating that cerebral ischemia-reperfusion injury could affect the pharmacokinetics

of 6-G in HGWD. After intragastric administration, 6-G can quickly penetrate the Blood-Brain Barrier (10 min) and reach the maximum concentration within 25 minutes, which is the same as reported in the literature.³⁰ 6-G has a small molecular weight, good fat solubility and high oil/water distribution coefficient is a factor of its extremely rapid absorption.

Conclusions

In conclusion, a microdialysis combined with UPLC–MS method was firstly developed and validated to investigate the pharmacokinetics of PF, CG, CC, and 6-G in the blood and brain of rats with cerebral ischemia injury following the administration of HGWD. The UPLC–MS/MS method fulfills all the required analytical characteristics for this purpose. The pharmacokinetics of PF, CG, CA, and 6-G were compared between the normal and cerebral ischemic rats following the intragastric administration of HGWD. The experimental results demonstrated that cerebral ischemic injury can affect the metabolism of drugs in the body, increasing the content of PF and 6-G and decreasing the content of CA and CG in the blood. Secondly, cerebral ischemic injury affected the apparent volume of distribution of PF and CA and the retention time of CG and 6-G in the brain. In normal and cerebral ischemic rats, the content of PF and 6-G was higher in the blood than in brain tissue, while CA and CG were increased in the brain tissue than blood, suggesting that CG and CA have high tissue distribution characteristics.

Funding

This work was supported by the National Natural Science Foundation of China (No. 81373973, No.81573872, No. 81873228), Discipline Research Characteristic Cultivation Project of Guangzhou University of Chinese Medicine (No. XKP2019004) and Science and Technology Planning Project of Guangdong Province (No. 2017KZDXM018).

Disclosure

Hao-Zhen Zheng reports grants from the National Natural Science Foundation of China, Discipline Research Characteristic Cultivation Project of Guangzhou University of Chinese Medicine, and Science and Technology Planning Project of Guangdong Province, during the conduct of the study. The authors report no other possible conflicts of interest in this work.

References

- Khandelwal P, Yavagal DR, Ralph L. Sacco. Acute ischemic stroke intervention. *J Am Coll Cardiol*. 2016;67:2631–2644. doi:10.1016/j.jacc.2016.03.555
- Lozano R, Naghavi M, Foreman K. 6-Global and regional mortality from 235 causes of death for 20 age groups in 1990 and 2010: A systematic analysis for the 6-global burden of disease study 2010. *Lancet*. 2012;380:2095–2128. doi:10.1016/S0140-6736(12)61728-0
- Li H, Guo J, Wang A, et al. Assessment of risk factors for cerebrovascular disease among the elderly in Beijing: A 23-year community-based prospective study in China. *Arch Gerontol Geriatr*. 2018;79:39–44. doi:10.1016/j.archger.2018.07.017
- Jiang W, Zhang FJ, Zao BH. Effect of Huangqi Guizhi Wuwu Decoction on patients with convalescent cerebral infarction. *World J Traditional Chinese Med*. 2017;12:1555–1559.
- Yin YX, Ren HQ. Treatment of 46 cases of sequelae of cerebral infarction with Huangqi Guizhi Wuwu Decoction. *Inner Mongolia Traditional Chinese Med*. 2017;36:11–14.
- Ma Y, Wang HW, Yang PP, Wang BL. Treatment of 80 cases of shoulder-hand syndrome after stroke with Huangqi Guizhi Wuwu Decoction combined with rehabilitation training. Chinese. *Med Mod Distance Educ*. 2016;14:76–80.
- Zhang LJ, Liu HK, Hsiao PC. New isoflavonoid glycosides and related constituents from astragali radix (*Astragalus membranaceus*) and their inhibitory activity on nitric oxide production. *J Agric Food Chem*. 2011;59:1131–1137. doi:10.1021/jf103610j
- Fu S, Gu Y, Jiang JQ, et al. Calycosin-7-O-β-D-Glucoside regulates nitric oxide/caveolin-1/matrix metalloproteinases pathway and protects blood–brain barrier integrity in experimental cerebral ischemia–reperfusion injury. *J Ethnopharmacol*. 2014;155:692–701. doi:10.1016/j.jep.2014.06.015
- Guo C, Tong L, Xi M, Yang H, Dong H, Wen A. Neuroprotective effect of calycosin on cerebral ischemia and reperfusion injury in rats. *J Ethnopharmacol*. 2012;144:768–774. doi:10.1016/j.jep.2012.09.056
- Ren M, Wang X, Du G, Tian J, Liu Y. Calycosin-7-O-β-D-6-Glucoside attenuates ischemia-reperfusion injury in vivo via activation of the PI3K/Akt pathway. *Mol Med Rep*. 2016;13:633–640. doi:10.3892/mmr.2015.4611
- Li S, Wang Y, Feng C, Wu G, Ye Y, Tian J. Calycosin inhibits the migration and invasion of human breast cancer cells by downregulation of Foxp3 expression. *Cell Physiol Biochem*. 2017;44:1775–1784. doi:10.1159/000485784
- Quan GH, Wang H, Cao J, et al. Calycosin suppresses RANKL-Mediated Osteoclastogenesis through Inhibition of MAPKs and NF-κB. *Int J Mol Sci*. 2015;16:29496–29507. doi:10.3390/ijms161226179
- Yu DH, Bao YM, Wei CL, An LJ. Studies of chemical constituents and their antioxidant activities from *Astragalus mongholicus* Bunge. *Biomed Environ Sci*. 2005;18:297–301.
- Fan Y, Wu DZ, Gong YQ, Zhou JY, Hu ZB. Effects of calycosin on the impairment of barrier function induced by hypoxia in human umbilical vein endothelial cells. *Eur J Pharmacol*. 2003;481:33–40. doi:10.1016/j.ejphar.2003.09.007
- Wu XL, Wang YY, Cheng J, Zhao YY. Calcium channel blocking activity of calycosin, a major active component of *Astragali Radix*, on rat aorta. *Acta Pharmacol Sin*. 2006;27:1007–1012. doi:10.1111/j.1745-7254.2006.00349.x
- Wang Y, Dong X, Li Z, Wang W, Tian J, Chen J. Downregulated RASD1 and upregulated miR-375 are involved in protective effects of calycosin on cerebral ischemia/reperfusion rats. *J Neurol Sci*. 2014;339:144–148. doi:10.1016/j.jns.2014.02.002
- Chen YF, Wu KJ, Wood WG. *Paeonia lactiflora* extract attenuating cerebral ischemia and arterial intimal hyperplasia is mediated by paeoniflorin via modulation of VSMC migration and Ras/MEK/ERK signaling pathway. *Evid Based Complement Alternat Med*. 2013;482428.

18. Wu YM, Jin R, Yang L, et al. Phosphatidylinositol 3 kinase/protein kinase B is responsible for the protection of paeoniflorin upon H₂O₂-induced neural progenitor cell injury. *Neuroscience*. 2013;240:54–62. doi:10.1016/j.neuroscience.2013.02.037
19. Cao BY, Yang YP, Luo WF, et al. Paeoniflorin, a potent natural compound protects PC12 cells from MPP⁺ and acidic damage via autophagic pathway. *J Ethnopharmacol*. 2010;131:122–129. doi:10.1016/j.jep.2010.06.009
20. Mao QQ, Zhong XM, Feng CR, Pan AJ, Li ZY, Huang Z. Protective effects of paeoniflorin against 6-glutamate-induced neurotoxicity in PC12 cells via antioxidant mechanisms and Ca²⁺ antagonism. *Cell Mol Neurobiol*. 2010;30:1059–1066. doi:10.1007/s10571-010-9537-5
21. Wang K, Zhu L, Zhu X, et al. Protective effect of paeoniflorin on Ab25–35-induced SH-SY5Y cell injury by preventing mitochondrial dysfunction. *Cell Mol Neurobiol*. 2014;34:227–234. doi:10.1007/s10571-013-0006-9
22. Nam KN, Yae CG, Hong JW, Cho DH, Lee JH, Lee EH. Paeoniflorin, monoterpene 6-Glycoside, attenuates lipopolysaccharide-induced neuronal injury and brain micro 6-Gial inflammatory response. *Biotechnol Lett*. 2013;35:1183–1189. doi:10.1007/s10529-013-1192-8
23. Zhang Y, Qiao L, Xu W, et al. Paeoniflorin attenuates cerebral ischemia-induced injury by regulating Ca/CaMKII/CREB signaling pathway. *Molecules*. 2017;22.
24. Wattanathorn J, Jittiwat J, Tongun T, Muchimapura S, Ingkaninan K. Zingiber officinale mitigates brain damage and improves memory impairment in focal cerebral ischemic rat. *Evid Based Complement Alternat Med*. 2011;2011429505.
25. Na JY, Song K, Lee JW, Kim S, Kwon J. Pretreatment of 6-shogaol attenuates oxidative stress and inflammation in middle cerebral artery occlusion-induced mice. *Eur J Pharmacol*. 2016;788:241–247. doi:10.1016/j.ejphar.2016.06.044
26. Longa EZ, Weinstein PR, Carlson S, Cummins R. Reversible middle cerebral artery occlusion without craniectomy in rats. *Stroke*. 1989;20:84–91. doi:10.1161/01.STR.20.1.84
27. Liao F, Meng Y, Zheng H, et al. Biospecific isolation and characterization of angiogenesis-promoting ingredients in Buyang Huanwu decoction using affinity chromatography on rat brain microvascular endothelial cells combined with solid-phase extraction, and HPLC-MS/MS. *Talanta*. 2018;179:490–500. doi:10.1016/j.talanta.2017.11.018
28. Zhang Y, Huo M, Zhou J, Xie S, Solver PK. An add-in program for pharmacokinetic and pharmacodynamic data analysis in microsoft excel. *Comput Methods Programs Biomed*. 2010;99:306–314. doi:10.1016/j.cmpb.2010.01.007
29. Tian X, Chen S, Zhang Y, et al. Absorption, liver first-pass effect, pharmacokinetics and tissue distribution of calycosin-7-O-β-d-glucopyranoside (C7G) and its major active metabolite, calycosin, following oral administration of C7G in rats by LC-MS/MS. *J Pharm Biomed Anal*. 2018;148:350–354. doi:10.1016/j.jpba.2017.10.027
30. Jiang SZ, Wang NS, Mi SQ. Plasma pharmacokinetics and tissue distribution of [6]-gingerol in rats. *Biopharm Drug Dispos*. 2008;29(9):529–537. doi:10.1002/bdd.638

Drug Design, Development and Therapy

Dovepress

Publish your work in this journal

Drug Design, Development and Therapy is an international, peer-reviewed open-access journal that spans the spectrum of drug design and development through to clinical applications. Clinical outcomes, patient safety, and programs for the development and effective, safe, and sustained use of medicines are a feature of the journal, which has also

been accepted for indexing on PubMed Central. The manuscript management system is completely online and includes a very quick and fair peer-review system, which is all easy to use. Visit <http://www.dovepress.com/testimonials.php> to read real quotes from published authors.

Submit your manuscript here: <https://www.dovepress.com/drug-design-development-and-therapy-journal>